A New Index For The Wintertime Southern Hemispheric Split Jet

Stella Babian[1], Jens Grieger[1], and Ulrich Cubasch[1]

[1]Meteorological Institute, Freie Universität Berlin, Carl-Heinrich-Becker-Weg 6-10, 12165 Berlin, Germany

Correspondence to: Stella Babian (stella.babian@met.fu-berlin.de)

Abstract. One of the most prominent asymmetric features of the southern hemispheric (SH) circulation is the split jet over Australia and New Zealand in Austral winter. Earlier studies developed indices to detect to which degree the upper-level mid-latitude westerlies are split and investigated the relationship between split events and the low-frequency teleconnection patterns Antarctic Oscillation (AAO) and El Niño-Southern Oscillation (ENSO). These different studies produced inconsistent results so that the relationships between the wintertime SH split jet and these climate variability indices remain unclear and are thus the scope of this study.

Up to now, all split indices are based on a definition, which focuses on a specific region where the jet split is recognizable. We consider the split jet as hemispheric rather than a regional feature and propose a new, hemispherical defined index: Our index is based on the principal components (PC) of the zonal wind field for the SH wintertime. A linear combination of PC2 and PC3 of the anomalous monthly (JAS) zonal wind is used to identify the split jet condition.

In a subsequent correlation analysis, our newly defined index (PSI) indicates a strong coherence with the Antarctic Oscillation (AAO). However, the significant relationship is unstable over the analysis period: During the 1980s the AAO amplitude was higher than the PSI and vice versa in the 1990s. It is supposed that the PSI, as well as the AAO, underlie low-frequency variability on the decadal to centennial time scales, but the analysis period is too short to draw these conclusions. A regression analysis with the Multivariate ENSO index points to a nonlinear relationship between PSI and ENSO, i.e. split jets occur during strong positive and negative phases of ENSO, but hardly under "normal" conditions. The PSA patterns, defined as the 2^{nd} and 3^{rd} mode of the geopotential height variability in 500 hPa, correlate poorly to the PSI ($r_{PSA-1} \approx 0.2$ and $r_{PSA-2} = 0.06$), but significantly to the individual components (PCs) of the PSI, uncovering an indirect influence on the SH split jet variability.

Our study suggests that the wintertime SH split jet is strongly associated with the AAO, while ENSO is to a lesser extent connected to the PSI. It is concluded that a positive AAO phase, as well as both flavors of ENSO and the PSA-1 pattern, produce favorable conditions for a SH split event.

1 Introduction

The circulation of the Southern Hemisphere (SH) is generally more zonally symmetric than its Northern Hemisphere counterpart, but there are still significant zonal variations in the upper-tropospheric time-mean flow. A unique asymmetric feature of the SH winter circulation is the climatological split jet over the longitudes of Australia and New Zealand (Fig. 1).

The split is composed of two well distinguishable branches: The northern branch, the subtropical jet (STJ) is located over the South Indian Ocean expanding to the South Pacific Ocean between the latitudes of 25° and 30° S. The STJ is paralleled by a weaker jet, the Polar Front Jet (PFJ), which is also concentrated in the south of Australia and over the South Pacific Ocean, but further poleward, near 60° S. A distinct feature of the split structure is a pronounced "gap" between these two branches, characterizing a zone of weak upper-level westerly winds over New Zealand (Bals-Elsholz et al., 2001).

Several past studies addressed the existence, location and variability of the wintertime SH split jet. An early study of Taljaard (1972) connected the existence and strength of the split jet to the outflow from the Asiatic monsoon anticyclone of the Northern Hemisphere. Further studies suggested that the split jet is associated with: Cold air outbreaks (Mo et al., 1987); the breakdown of the Antarctic polar vortex in late spring (Mechoso et al., 1988) or the phase of the El Niño-Southern Oscillation (ENSO) (Karoly, 1989; Chen et al., 1996) and the Antarctic Oscillation (AAO) (Yang and Chang, 2006).

The AAO, which is in literature also referred to as Southern Annular Mode (SAM), is the dominant climate mode of the extra-tropical SH circulation variability and describes the out-of-phase pressure anomalies in polar and mid-latitude regions (e.g. Lorenz and Hartmann (2001), Thompson and Wallace (2000)). Positive (negative) phases of the AAO are linked to a poleward (equatorward) shift and strengthening (weakening) of the PFJ. The AAO was found to be the main modulator of the PFJ strength and location (Limpasuvan and Hartmann, 1999) and is thus expected to play a major role in the split jet formation. The ENSO has an impact on both, STJ and PFJ by directly acting on the Hadley circulation: While El Niño events are connected to increased (equatorial) convection and a stronger Hadley cell, which in turn enhances the STJ and simultaneously weakens the PFJ, La Niña phases are marked by a stronger (weaker) PFJ (STJ) (Karoly, 1989; Chen et al., 1996; Kitoh, 1994). Gallego et al. (2005) affirmed that the ENSO impact on attributes of the PFJ (strength, wavenumber, average latitude) is mainly confined to the Pacific sector, where the split jet is located.

Bals-Elsholz et al. (2001) developed a vorticity based split index and investigated the relation to both, ENSO and the AAO. Their study reveals that the existence of the split jet depends highly on the presence of the PFJ part, given that the STJ is a quasi-permanent feature of the SH winter circulation. The PFJ part of the split index is indeed correlated to the AAO, while the STJ part shows no correlation. Thus, in total their index correlates weakly to the AAO. A later study (Inatsu and Hoskins, 2006) suggested a split index based on zonal mean zonal wind variations. It correlates low ($r = 0.43$), although significant to the AAO. Both studies also investigated the relation to ENSO: Neither the index from Bals-Elsholz et al. (2001) nor the one developed by Inatsu and Hoskins (2006) correlated on a significant level to the Southern Oscillation Index (SOI).

The controversy about the relations between AAO, ENSO and the SH split jet among these studies led to the question: Can an index be defined which clarifies the relationships between the SH split jet and the large-scale teleconnection indices ENSO and AAO?

In both formerly studies (Bals-Elsholz et al. (2001) (hereafter BE), Inatsu and Hoskins (2006) (IH)) and in the work of Yang and Chang (2006) (YC) indices were developed to detect the characteristics of the SH climatological split in Austral winter. These indices represent the split structure in several meteorological variables and in different but comparable levels: 200 hPa vorticity (BE), 300 hPa zonal wind anomalies (YC), 200 – 300 hPa difference in the zonal mean zonal wind (IH). The mutuality in the construction of all these split indices is a definition based on the regions accounting for the two branches of the split

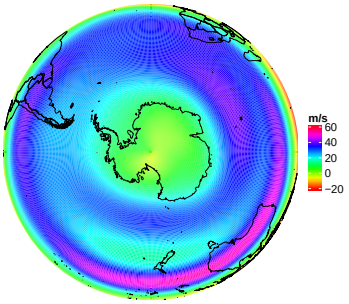

Figure 1. Climatological zonal wind (m/s) in 200 hPa in Austral winter (JAS) averaged for the period 1979–2015.

jet (STJ, PFJ) and the gap between those over the Australian / New Zealand region. Although these indices are constructed similarly, the respective studies revealed inconsistent relations to the AAO and ENSO.

Additionally, the literature lacks a description of whether the split jet variability is related to the Pacific South American (PSA) patterns, although these were found to be associated with both teleconnection indices, ENSO and the AAO. The PSA patterns are conventionally seen as Rossby wave trains emanating in quadrature to each other from the tropical Pacific towards Argentina and serve simultaneous as waveguide for eddies moving south. On interannual time scales the PSA-1 mode is tied to ENSO, while the PSA-2 pattern is associated with the quasi-biennial component of ENSO (e.g., Mo, 2000). Furthermore, although called an "annular" mode, the AAO contains asymmetries, which are most pronounced in Austral winter and over the Pacific sector. This (tropically forced) component of the AAO is related to a fixed active Rossby wave source and resembles the spacial structure of the PSA patterns (Ding et al., 2012).

The lack of knowledge about the relationship between the split variability and the PSA patterns and the inconsistencies among earlier studies concerning the connections to ENSO and the AAO motivate the development of an improved SH split jet index. The split jet is one of the most important features of the interannual variability in the SH winter circulation and its pattern is not only centered over the Australian / New Zealand region but bears also hemispheric signatures (Yang and Chang, 2006). Consequently, we assume that the split jet variability is already intrinsically contained in one or several leading modes of the SH winter zonal wind field.

In this study, we provide a PC based methodology to describe the SH wintertime split jet in order to clarify the relations between the SH split jet and the large-scale teleconnection indices ENSO and AAO. This paper is organized as follows: The data set and methodology used for the reconstruction of the split jet indices and for the calculation of the new PC based split index (PSI) are introduced in the data and methods Section 2. The definition of the new index is proposed in Section 3. We will use the PSI to examine the relations between split phases to the known large-scale variability modes (ENSO, AAO and PSA) in Section 4. Finally, the main results are summarized and discussed in Section 5.

2 Data and methods

2.1 Data

This study makes use of the ERA-Interim (Dee et al., 2011) reanalysis data sets from the European Centre for Medium Range Weather Forecast (ECMWF). ERA-Interim was selected because ECMWF products (e.g. MSLP and geopotential height in 500 hPa from ERA-Interim) were found to be the most reliable data, in particular over the Antarctic continent (Bracegirdle and Marshall, 2012).

We use monthly zonal wind an geopotential height data covering the winter seasons, defined here for the months from July to September (JAS) in accordance with the three studies mentioned above. All fields were used on a 0.75° grid and were analyzed for the period from 1979–2015.

The monthly resolved teleconnection indices used in this study, namely the Antarctic Oscillation Index and the Multivariate ENSO Index, are both freely available from NOAA's website (http://www.noaa.gov/).

All time series used in this study are standardized so that they have a mean of zero and a standard deviation of one.

2.2 Empirical Orthogonal Function (EOF) Analysis

Analysis of atmospheric circulation patterns can be done by means of an Empirical Orthogonal Functions Analysis (EOF), which is also referred to as Principal Component Analysis (PCA) (Jolliffe, 2002; Hannachi et al., 2007). By definition, an EOF analysis reduces a data set containing a large number of variables to a data set containing fewer new variables, which are linear combinations of the original ones (Wilks, 2011). The first principal component (PC) is the linear combination with the largest variance.

To analyze the variability of the SH zonal wind we first removed the seasonal cycle by taking the anomalies with respect to a mean annual cycle which was obtained by an average of the individual winter months of the year. The individual grid cells are then centered and scaled with the square-root of their latitude to account for different grid cell sizes. We then performed an EOF analysis of the 111 winter months from the period 1979–2015. The associated PC gives the respective time series.

By definition, the PSA modes are the 2^{nd} and 3^{rd} EOF of the 500 hPa geopotential height anomalies over the SH (Mo, 2000). The associated PCs give the PSA-1 (2^{nd} PC) and PSA-2 (3^{rd} PC) time series.

2.3 Composite and Correlation Analysis

Composites of months with an anomalous high or low split index are the basis for investigating the potential mechanisms associated with splits in the time-mean SH winter circulation. Monthly values exceeding (undercutting) the respective normalized index mean (1979–2015) about plus (minus) one standard deviation (Hendon et al., 2007) were averaged and defined as positive (negative) composite. To quantify the linear relationship between the split jet time series and several indices of the known large-scale oscillations (i.e. AAO and ENSO) the Pearson's correlation coefficient is evaluated (Wilks, 2011).

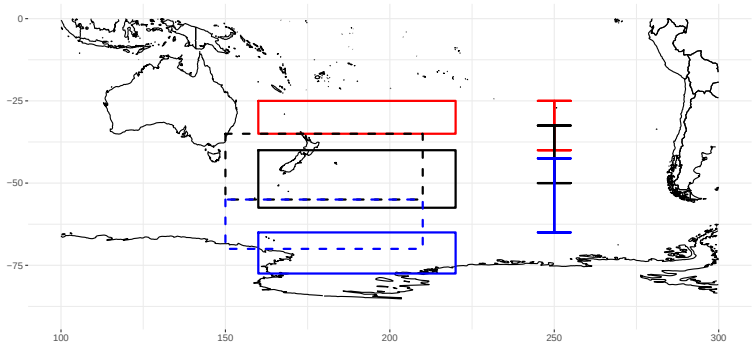

Figure 2. Area definitions of three earlier studies. Red lines show the STJ part, blue lines the PFJ part and the black lines the gap between the two branches defined by the different studies. Continuous lines refer to the SFI of Bals-Elsholz et al. (2001) and dashed lines mark the two regions defined in Yang and Chang (2006). The right side shows the meridional boundaries used in the split index defined by Inatsu and Hoskins (2006).

2.4 Split Jet Index Definitions

Fig. 1 shows the 200 hPa climatological SH winter (JAS) zonal mean wind and the typical time-mean split jet, composed of a subtropical (at 30° S) and a polar branch (roughly at 60° S) as well as the characteristic zonal wind minimum in between.

The three split jet indices which were introduced in the introduction are based on flow characteristics for the specific regions of Australia and New Zealand (see Fig. 2). Each index is based on a Subtropical Jet (STJ) and a Polar Front Jet (PFJ) component and a gap between these two branches, except the YC index, which lacks the subtropical part. Table 1 provides information about these areas and gives an overview of the particular data sets used in the split jet references.

2.4.1 Split-flow Index (SFI)

Bals-Elsholz et al. (2001) developed the very first split index to evaluate the structure and evolution of the SH split jet structure. A Split-Flow Index (SFI) based on the relative vorticity (ζ) in 200 hPa in three neighboring regions (Fig. 2) was designed as follows:

$$SFI = \zeta_{PFJ} + \zeta_{STJ} - \zeta_{GAP} \tag{1}$$

The normalized monthly index gives large negative (positive) values for split (non-split) years. Split flow regimes similar to the climatological mean have normalized SFI values near zero.

	SFI (BE)	STJ (YC)	STJ (IH)	PSI
Reference	Bals-Elsholz et al. (2001)	Yang and Chang (2006)	Inatsu and Hoskins (2006)	Defined within this study (Sec. 3.2)
Data sets				
Variable	relative vorticity	zonal wind	zonal mean wind	zonal wind
Level	200 hPa	300 hPa	mean of 200 and 300 hPa	200 hPa
Data Source	NCEP NCAR	ERA15	ERA40	ERA-Interim
Period	1958 – 2000	1979 – 1993	1979 – 2001	1979–2015
Regions used for definitions				
STJ	25 – 35° S	–	25 – 40° S	SH
GAP	40 – 57.5° S	35 – 55° S	32.5 – 50° S	
PFJ	65 – 77.5° S	55 – 70° S	42.5 – 65° S	

Table 1. List of split jet definition constraints as suggested in three earlier studies. The indices resemble specific areas depicting the equatorward branch of the split (STJ), the gap between the jets (GAP) and the Polar Front Jet part (PFJ).

2.4.2 Normalized Monthly Split-Jet Index (NMSJI)

The Yang and Chang (2006) Split Jet Index (SJI) is based on the difference in 300 hPa time-mean zonal wind anomalies (U) in two adjoining areas (PFJ, GAP). The index is normalized then by subtracting the climatological mean and by dividing its standard deviation.

$$SJI = \overline{U}_a^{PFJ} - \overline{U}_a^{GAP} \tag{2}$$

$$NMSJI = \frac{MSJI - \overline{MSJI}}{\sigma} \tag{3}$$

2.4.3 Split Jet Index (SJI)

The Split Jet Index published by Inatsu and Hoskins (2006) was defined as the difference of the 200 hPa and 300 hPa zonal mean zonal wind (U) between the (overlapping) latitudinal boundaries given in Tab. 1 and illustrated in Fig. 2.

$$SJI = U_{STJ} - 2 \cdot U_{GAP} + U_{PFJ} \tag{4}$$

In agreement with the weighting of the wind minimum between the jets by 2, the index values rise for both, a strong STJ and/or PFJ and reduce or even reverse if there is a strong single jet centered in the (gap) region between the two jets.

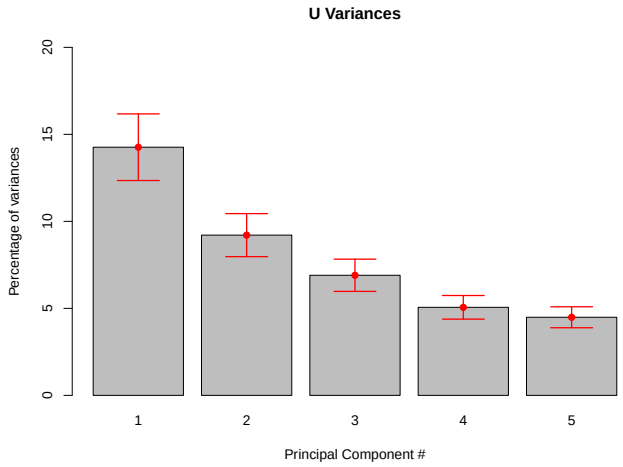

Figure 3. Proportions of the total variance [%] associated with the leading 5 EOFs for the 200 hPa zonal wind field of ERA-Interim reanalysis. Error bars are estimates of sampling errors in EOF computation according to "North's rule of thumb" (North et al., 1982).

3 A new index for the wintertime SH split jet

As mentioned previously, the wintertime split jet is the most prominent asymmetric feature of the mid-latitude SH circulation centered over the Pacific sector although it bears as well hemispheric signatures (Yang and Chang, 2006). In order to design a PC based split jet index, three earlier defined split jet indices (Section 2.4) were reproduced and their respective statistical relationships to the leading modes of the SH wintertime circulation (as depicted by zonal wind anomalies at 200 hPa) have been investigated in this section. The EOF modes showing the largest coherence with the split jet indices (as defined by the respective studies) are assumed to contain the main signals associated with the split variability.

3.1 EOFs in SH zonal wind

The three leading spatial patterns of variability (EOFs) for U 200 hPa anomalies on the SH (0–90° S) account for roughly 14%, 9% and 7% of the total variability of the 200 hPa zonal wind field (Fig. 3). The 200 hPa pressure level was chosen due to the mechanisms associated with the jet(s) variability, which have their maximum at that level (e.g., Galvin, 2007). The subsequent EOFs (higher than the 3^{rd}) represent about 5% and less of the total variability and are not distinguishable from each other after "North's rule of thumb" (North et al., 1982).

The correlation between the leading 5 PCs and the split indices introduced earlier is shown in Tab. 2. PC1 correlates significantly (r = -0.49) with the zonal mean zonal wind based index developed by Inatsu and Hoskins (2006) and weakly although significant to the relative vorticity based index designed by Bals-Elsholz et al. (2001). The weaker correlation to the Yang and Chang (2006) index, which is also defined in zonal wind accounts from the fact, that this SJI lacks the STJ part.

	PC1	PC2	PC3	PC4	PC5	PSI
JAS – correlation values						
-BE	**-0.28**	**0.44**	**-0.36**	-0.09	-0.15	**0.56**
YC	-0.24	**0.56**	**-0.48**	-0.13	-0.09	**0.73**
IH	**-0.49**	**0.57**	**-0.43**	**0.26**	0.09	**0.71**
Mean	**-0.38**	**0.59**	**-0.48**	0.02	-0.05	**0.76**

Table 2. Monthly (JAS) Pearson correlation coefficients of individual leading 5 PCs in the 200 hPa zonal wind as well as the PSI with the split jet indices introduced in the methods section (Sec. 2). By construction, the Bals-Elsholz et al. (2001) index becomes negative during split events and its sign is therefore reversed. Bold values are significant at the α = 1% level.

Whereas the 4^{th} and 5^{th} PC correlate poorly with any of the indices, the 2^{nd} and 3^{rd} PC show robust relations to split events. While PC2 is strongly positively correlated to the split indices with coefficient values ranging from r = 0.44 (BE) to r = 0.57 (IH), PC3 is negatively related to the split regimes: Pearson's correlation values of PC3 raise from r = -0.36 (BE) to r = -0.48 (YC). Generally, the correlation values associated with the relative vorticity based index designed by Bals-Elsholz et al. (2001) show the weakest links to PC2 and PC3 of the zonal wind field, but are however significant at the α = 1% level.

The two zonal wind-based indices (IH and YC) produce the strongest correlations to PC2 and PC3, which is excelled only by the mean of all three earlier split indices for PC2 (r = 0.59). Altogether, the splits in the westerlies are less correlated to PC1, but are rather associated with the higher order PCs in the 200 hPa zonal wind field.

3.2 Definition of the PC based Split Index (PSI)

From the correlation analysis with three discussed split indices it is apparent, that PC2 and PC3 are associated with the SH wintertime split jet events and resemble the partly split variability. In order to develop a PC based split jet index, these PCs, correlating well with the earlier split jet indices, are coupled to a linear combination. Consequently, the monthly wintertime (JAS) PC based SH Split Jet Index (PSI) is defined as follows:

$$PSI = PC2_{U_{200hPa}} - PC3_{U_{200hPa}} \tag{5}$$

The PSI is based on the 2^{nd} and 3^{rd} PC of the anomalous 200 hPa zonal wind field over the whole SH during Austral winter (JAS). The PSI time series, as well as the split indices of the previous studies, are displayed in Fig. 4.

The correlation values between these indices and the PSI in 200 hPa are shown in the last column of Tab. 2. All indices are well correlated to the PSI with coefficients ranging from 0.56 (BE) to 0.73 (YC) and the mean of all the three earlier split indices raises Pearson's correlation coefficient to r = 0.76. This relationship is significant at the α = 1% level and shows that the linear combination of PC2 and PC3 exceeds the relation compared to the performance of the individual PCs (Tab. 2).

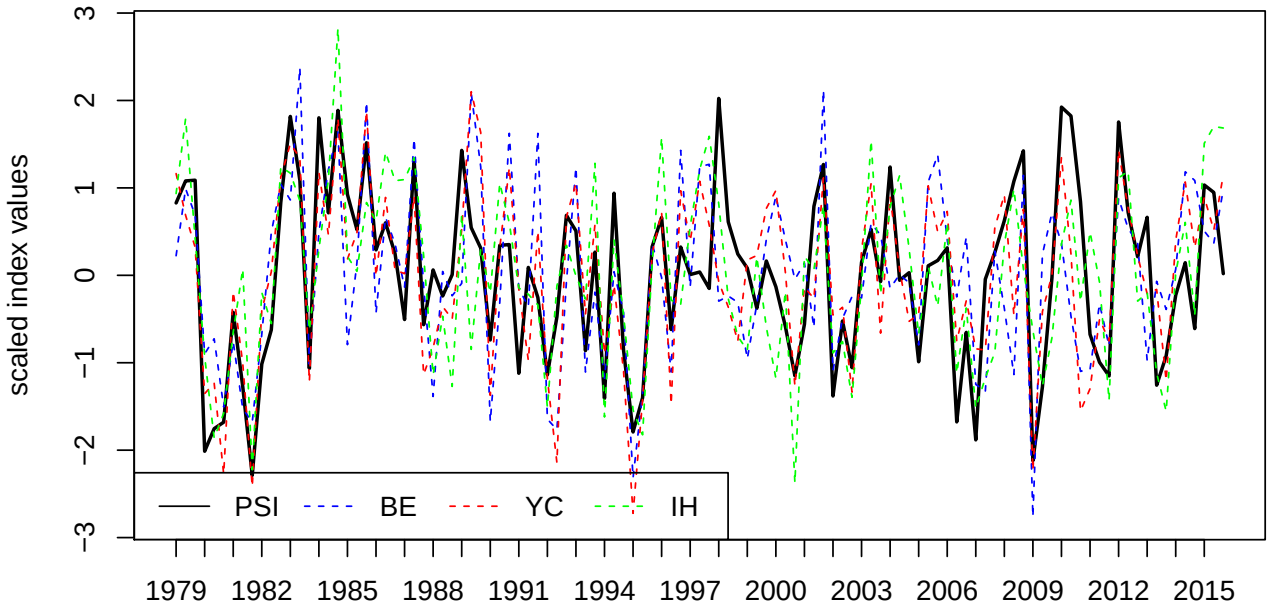

Figure 4. PSI (PC2-PC3) index in 200 hPa zonal wind and three earlier split jet indices defined by Bals-Elsholz et al. (2001) (BE), Yang and Chang (2006) (YC) and Inatsu and Hoskins (2006) (IH). All time series were scaled for illustration purposes.

4 Results

4.1 Composite Analysis of U 200 hPa with PSI

Fig. 5 shows the spatial patterns of U in 200 hPa for high (18 cases) and low (19 cases) PSI index phases. The positive composite affirms the characteristic split structure with an existing, but weak STJ, a pronounced PFJ and a well-defined minimum of zonal wind strength in between. The split composite shows that the PFJ strength is not limited to the Australian sector of the east Pacific, but is enhanced from the Indian Ocean over the full width of the South Pacific Ocean. The low index composite displays a clear non-split or "merged" jet state with a strong STJ over the Australian continent and a missing PFJ. The spatial patterns of the split and non-split cases are well captured by the PSI and show similar results to the composites of the indices defined in Section 2.4 (not shown).

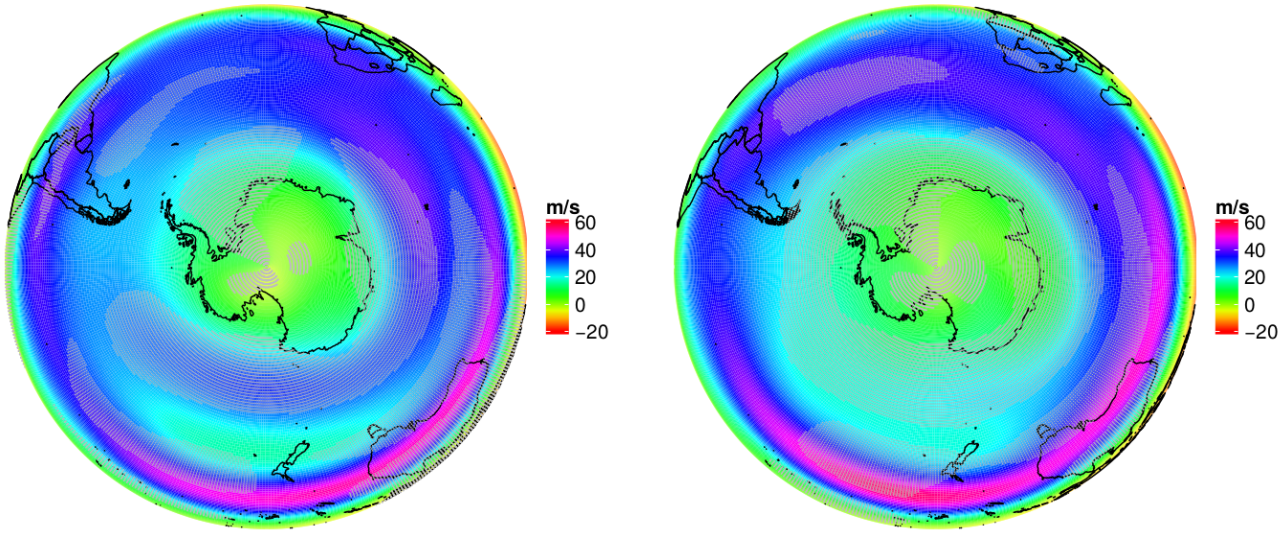

Figure 5. Positive (left) and negative (right) composite of the PSI (PC2-PC3) index in 200 hPa zonal wind. Gray dotted areas are significant at the α = 1% level.

To understand the contribution of both components of PSI, i.e. PC2 and PC3, a composite study of both PCs was also done separately. Fig. 6 shows the appropriate composites of the 2^{nd} and 3^{rd} EOF in U 200 hPa. Please note that the plots in Fig. 6 are arranged in such a way, that the left column refers to the split condition and the right column to the non-split phase. The positive composite of PC2 shows the typical split, which was developed over the Indian Ocean and strengthened in the western Pacific sector where a clear double jet structure with a pronounced minimum in U 200 hPa between the two jets is visible. Crosswise, the negative composite of PC2 displays a single jet formation (right column).

The bottom row of Fig. 6 gives the equivalent composites of PC3. The most striking difference in the split composites (Fig. 6, top left) is the PFJ strength over the western Pacific Ocean and the Drake Passage, which lacks in the PC2 composite. Compared to PC2, where the PFJ blends over the central Pacific, the PFJ reinforces and establishes a double jet structure over the Atlantic Ocean, which breaks down south of South Africa and results in a strong STJ again (Fig. 6, bottom left). A further feature of the positive composite is the lack of annular structure compared to PC2. In literature, this known zonal wave number 3 pattern is often referred to as a modulator of e.g. Blocking events in the New Zealand region and Australian rainfall (Trenberth and Mo, 1985; Pook et al., 2013).

The negative composite (Fig. 6, bottom right) of the second term of Eq. 5, i.e. -PC3 (non-split / single jet regime) bears resemblance to the appropriate composite of PC2 but describes a stronger STJ over the central and east South Pacific Ocean

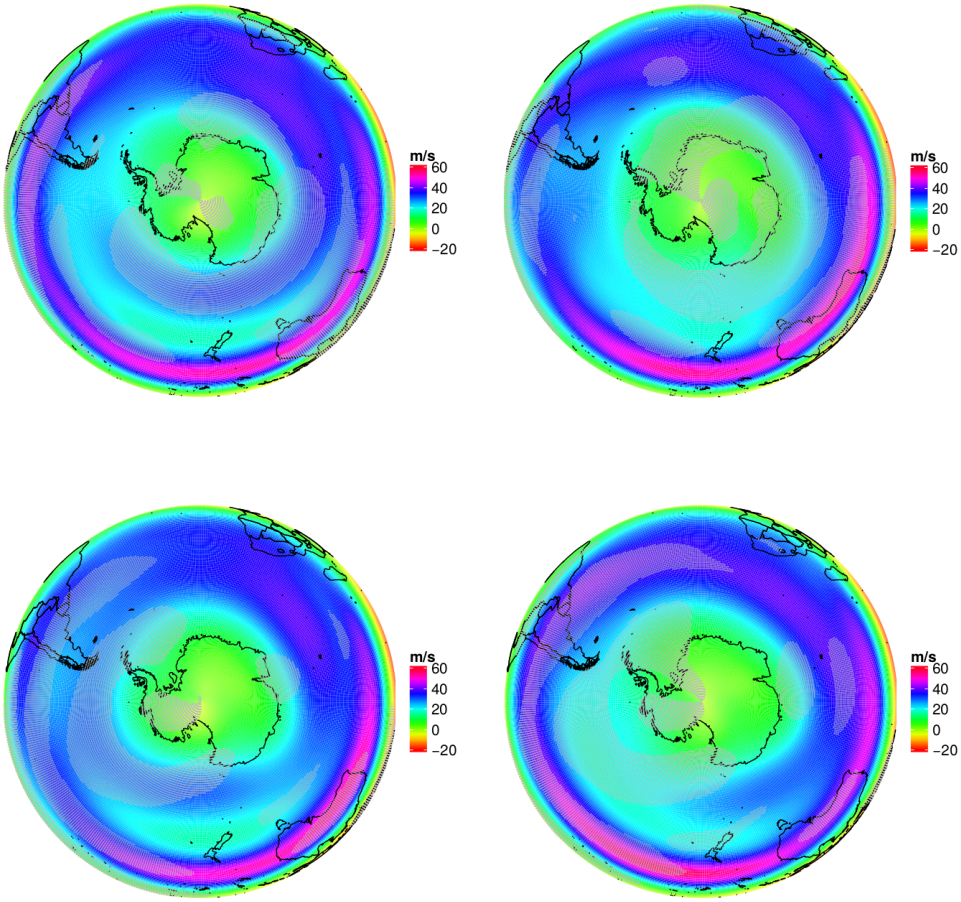

Figure 6. Composites of positive (left) and negative (right) phases of PC2 (first summand of Eq. 5; top row) and -PC3 (second summand of Eq. 5; bottom row) time series of the SH zonal wind in 200 hPa. Gray dotted areas are significant at the α = 1% level.

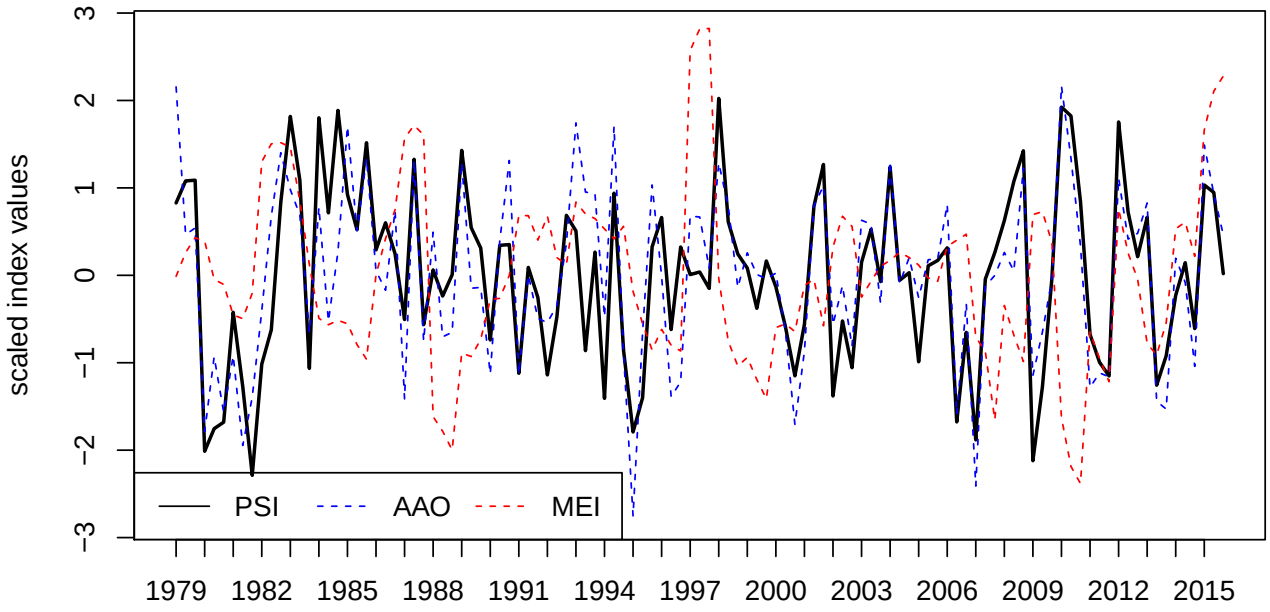

Figure 7. Time series of PSI (black solid line), NOAA's AAO (blue dotted line) and NOAA's MEI (red dotted line) from 1979 to 2015.

and South America. Additionally, the PFJ is weakened in the non-split composite, but south of the Australian / New Zealand region there are still traces of a PFJ.

In summary, the positive PSI composite (Fig. 5 left) benefits from the combination of the double jet structure with a pronounced minimum between the jets associated with PC2(+) and the strong PFJ over the South Pacific Ocean associated with the "non-annular" component localized over the South Pacific Ocean of PC3(-).

4.2 Links between PSI and large-scale climate modes (AAO, ENSO and PSA)

In order to determine whether the PSI is modulated by large-scale phenomena, i.e. the Antarctic Oscillation (AAO) and the El Niño-Southern Oscillation (ENSO), correlations between the PSI and the teleconnection indices are computed. The respective time series are illustrated in Fig. 7 and Pearson's correlation coefficients, based on 111 winter months, are summarized in Tab. 3.

	PSI	PC2	PC3	BE	YC	IH	Mean
JAS – correlation values							
AAO	**0.81**	**0.65**	**-0.50**	**0.45**	**0.66**	**0.58**	**0.64**
MEI	-0.09	0.07	0.20	0.20	0.12	**0.34**	**0.25**
PSA-1	0.19	**-0.26**	**-0.55**	0.14	0.16	-0.17	0.05
PSA-2	0.06	0.20	0.13	0.22	0.20	-0.12	0.11

Table 3. Monthly (JAS) Pearson correlation coefficients of the three split indices introduced in the methods section, as well as the PSI with three major SH climate mode indices for the Antarctic Oscillation (AAO), ENSO (Multivariate ENSO Index) and the Pacific South American (PSA) patterns (PSA indices as defined in Mo (2000) for PSA-1 and PSA-2). Bold values are significant at the α = 1% level.

The Antarctic Oscillation (AAO), in literature also referred to as the Southern Annular Mode (SAM), is defined here as the anomalous geopotential height in 700 hPa (NOAA's AAO) and describes the out-of-phase pressure anomalies in polar and mid-latitude regions (e.g. Lorenz and Hartmann (2001), Thompson and Wallace (2000)). The correlation analysis reveals a powerful connection (r = 0.81) between the PSI (defined in 200 hPa) and the AAO. The highly significant correlation value accounts for the large influence of the AAO to the PFJ variability, which in turn is associated with the regime of the jets (Fyfe (2003), Gallego et al. (2005)).

Although there is a significant correlation to the AAO proposing a strong link to the PSI variability, there is no such relation to the Multivariate ENSO Index (MEI). Fig. 8 shows a regression of the monthly MEI values in dependence on the respect PSI value. The correlation value between the PSI and MEI is low (r = 0.04), but by comparing the top left and the top right quadrant of the scatter plot (Fig. 8) to the respective bottom quadrants it is evident that warm (red dots) and cold (red dots) ENSO events are both associated with positive (or neutral) values of the PSI. Altogether, from 24 warm and cold ENSO events as occurred in 111 winter months, there was no month with a negative PSI value. This asymmetric and nonlinear behavior damps the correlative relation.

Tab. 4 gives counts of positive (first column), negative (second column) and neutral (last column) PSI months and the corresponding predominant AAO and ENSO states. The box, which emerges when concentrating on the first six lines and columns of the same table, contains all possible AAO^+/PSI^+ and AAO^-/PSI^- cases during the analysis period. Although the AAO index is well correlated to the PSI, the last column of the same table bears that 5 AAO^+ months are marked as neutral PSI months, while there are 5 months of PSI^+ and neutral AAO conditions. Consequently, the jet is able to split under neutral AAO conditions and not every AAO^+ month leads compulsorily to a split event. The negative phases of the AAO nearly mirror the conditions of its positive counterpart. Altogether 7 events occurred under AAO^-/PSI^0, likewise, 6 months were counted as AAO^0/PSI^- cases.

By revisiting these points in the investigated period from 1979 to 2015 it turns out that 3 months of the first case (AAO^+/PSI^0) occurred in a period during the 1980s and 3 of the latter cases (AAO^0/PSI^+) build a sequence in the 1990s (not shown). A spectral analysis of the time series of the differences between PSI and AAO index shows multiple frequencies over the 37 year

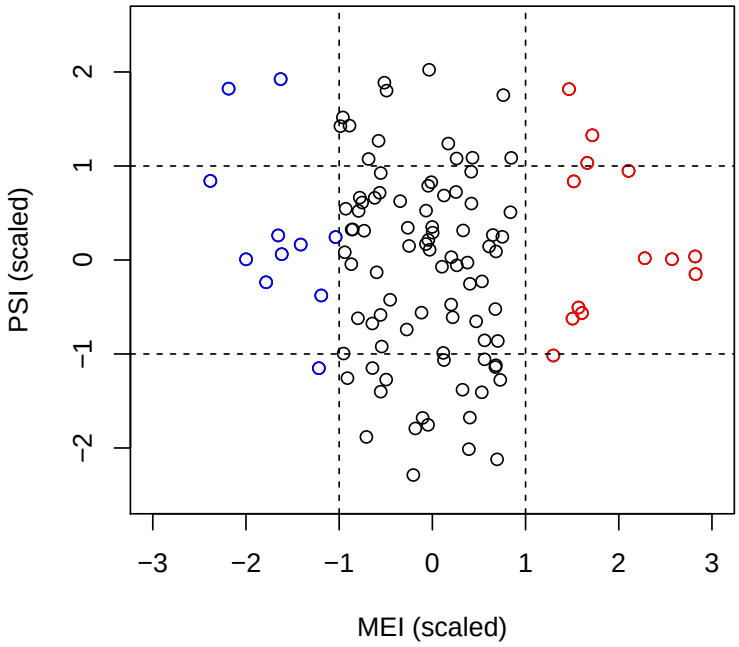

Figure 8. Scatter plot of the new split index (PSI) and MEI, the Multivariate ENSO Index (each normalized to unit variance). Dashed lines give (minus) one standard deviation of MEI and PSI indices, respectively. Red (blue) dots mark warm (cold) ENSO events.

Combination	PSI^+	PSI^-	PSI^0
AAO^+ MEI^+	3	–	–
AAO^+ MEI^-	2	–	–
AAO^+ MEI^0	8	–	5
AAO^- MEI^+	–	–	1
AAO^- MEI^-	–	1	–
AAO^- MEI^0	–	12	6
AAO^0 MEI^+	2	–	7
AAO^0 MEI^-	–	–	8
AAO^0 MEI^0	3	6	47

Table 4. The predominant jet regimes (PSI^+ = split jet, PSI^- = single jet, PSI^0 = mixed jet regime) as counted during the 111 winter months of the 1979–2015 period, separated by occurred combinations of AAO and ENSO states.

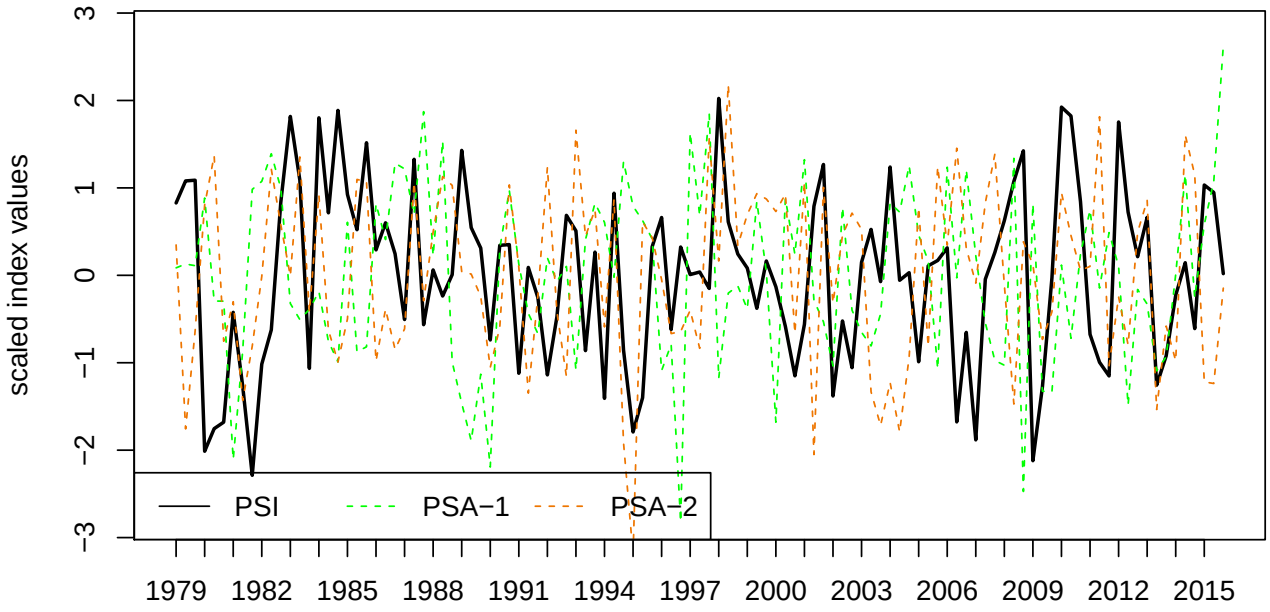

Figure 9. Time series of PSI (black solid line), PSA-1 index (green dotted line) and PSA-2 index (orange dotted line) from 1979 to 2015.

long period (not shown). Unfortunately, the time series is too short to draw meaningful conclusions about decadal to centennial variabilities. Furthermore, the time series of differences is neither correlated to ENSO nor to the well known Pacific Decadal Oscillation (NOAA's PDO index, not shown).

The low correlative relationship between MEI and PSI mentioned above arises from the fact, that 8 out of 18 split events occurred during any flavor of ENSO phases, while only one cold ENSO event occurred in a negative PSI phase. The last three rows of Tab. 4 reveal that there are 7 (8) ENSO warm (cold) events, thereof the extreme La Niña event in 1988 and the severe El Niño event from 1997, where a mixed jet (PSI^0) regime predominated.

Fig. 9 shows the time series of both PSA modes and the PSI. Although the correlation between PSI and the PSA indices is low (r_{PSA-1} = 0.19 and r_{PSA-2} = 0.06), the PSA-1 mode is significantly correlated to the individual PCs of the SH zonal circulation variability (Tab. 3). Both PSI components (i.e. PC2 and PC3) are associated to the PSA-1 pattern. The spacial pattern of EOF2 was previously identified to resemble the dominant part of the split jet structure (Section 3.1) marked by an intensified PFJ over the eastern hemisphere. Since the PSA-1 pattern is primary associated with the variability over the central and western Pacific sectors, it can be concluded that PC2 describes less PSA-1 variability but contains a considerable part of

the wind response associated with the AAO. PC3 accounts for the "non-annular" component of the PSI and contains most variability over the Pacific sector. It is argued, that PC3 contains remarkable PSA-1 variability. However, only 3 cases were identified where both indices, PSI and PSA-1, exceeded the threshold of one standard deviation during the analysis period (not shown).

5 Summary and discussion

While many previous studies of the SH winter circulation examined the presence, origin and structure of the climatological time-mean SH split jet, which establishes over the western South Pacific Ocean in the vicinity the South Australia / New Zealand region, only a few studies developed indices capturing the SH split variability to quantify the relations to the large-scale variabilities, i.e. the Antarctic Oscillation (AAO) and the El Niño-Southern Oscillation (ENSO).

According to our literature review, up to now there are three (past) studies suggesting a SH split jet index. All indices use a region based definition, which contradicts the assumption, that the SH split jet is a hemispheric feature rather than a regional effect. The most important advantage and the novelty of our new PC based split index (PSI) compared to the existing indices, is its independence from regional definitions: The PSI is defined by linearly combining the SH 2^{nd} and 3^{rd} principal component of the monthly (JAS) anomalous zonal wind in 200 hPa.

The PSI correlates well to the individual split indices and the mean of all gives a significant correlation coefficient of 0.76 to the PSI. An analysis of Bals-Elsholz et al. (2001) showed, that their SFI agreed favorably with a subjective classification of the split regime, with the exception of 1998. This year was affected by a strong La Niña event and an anomalously weak STJ. While the three earlier split indices failed to agree with the (subjective) split regime, the PSI value for July 1998 was high and thus marked as one of 18 split events. From this fact, from the correlation analysis and the investigation of PSI composites in the 200 hPa zonal wind field it is evident, that our PC based split index is able to reproduce the SH wintertime split jet structure.

Separate composites of PC2 and PC3 reveal that both PCs are essential for the split representation. PC2 is associated with the jet strength (Lorenz and Hartmann, 2001) over the eastern hemisphere, whereas PC3 exhibits a "non-annular" component in both composites. It is reasoned that split events are connected to PC2 because it represents the jet strength and to PC3, as it adds a "non-annular" component to the jet variability. Thus, the PC based split jet index (PSI) is a qualitative measure of the spatio-temporal variability of the split jet and can efficiently be used to investigate the relationships to the known climate variability modes, i.e. AAO, ENSO and PSA patterns.

Although not demonstrated in earlier studies concerning the SH circulation (jet) variability (e.g. Gallego et al. (2005)) it was expected that the SH split jet exhibits a solid connection to the AAO. The new PSI shows a highly significant correlation to the leading mode in a near-surface level of the geopotential height anomalies (NOAA's AAO in 700 hPa) with r = 0.81. This highly significant relation of the PSI to the leading mode in geopotential reiterates the importance of the AAO to the PFJ variability (Fyfe (2003), Gallego et al. (2005)). The PFJ strength is enhanced under AAO^+ conditions in accordance with the negative pressure anomalies over the polar region occurring under AAO^+. Since the PFJ variability is more important for the representation of split events (Bals-Elsholz et al., 2001) than its subtropical counterpart, the AAO has a high correlation with

the PSI (0.81). Nevertheless, there are 5 out of 18 split events occurring in the analysis period of 1979–2015, where the AAO index had a neutral value. It can be concluded that a positive AAO phase is a preferred condition for the SH split jet, however, the split jet is also able to arise in neutral AAO months.

The correlation between the Multivariate ENSO Index (MEI) to the PSI is low, but 7 out of 18 split events occurred during a warm (5) or cold (2) ENSO month. The occurrence of both, warm and cold ENSO events damps indeed the correlation value to the PSI, but the relative frequency of ENSO events is still 30%. It seems likely that any kind of ENSO flavor is favorable for split events, which results in a nonlinear relation between PSI and ENSO, i.e. that positive (negative) PSI values mainly occurred during warm or cold (neutral) ENSO states. From earlier studies it is well known, that El Niño (La Niña) phases enhance (reduce) the STJ strength over the South Pacific Ocean via advection of mean flow momentum flux (e.g. Chen et al. (1996)). This is consistent with our finding that 5 out of 18 split events occurred during a warm ENSO phase, which enhances the STJ (PFJ) strength. Otherwise, there are strong ENSO events (El Niño of 1997 and La Niña in 1988) during the analysis period, which did not lead to a pronounced split event. Thus, an ENSO event alone is not able to reproduce the SH split jet variability. Worth mentioning, in literature it is well known that ENSO and AAO are in turn not independent from each other. There are hints that cold ENSO events are favored by positive phases of the AAO (e.g. Carvalho et al. (2005)). As these are in turn associated with split events, we expected La Niña phases to occur more often than El Niño events during PSI^{+} phases. Contrastingly, the ENSO warm phase coincided more frequent (5 months) with the high PSI (split jet) phases than its cold counterpart (2 months), although both flavors of ENSO appeared roughly equally during the considered time period of 111 winter months. It is reasoned that the ENSO induced Rossby wave dynamics are beneficial for the SH split jet modulation, regardless of the sign of that oscillation. However, further work is needed here to clarify the complex relationship between ENSO and the SH split jet.

The traditional perception suggests that the PSA patterns are part of a stationary Rossby wave train extending from the central Pacific to Argentina (e.g., Mo and Higgins, 1998). The PSA patterns, typically defined as 2^{nd} and 3^{rd} modes of tropospheric geopotential height variability over the SH (e.g., Mo, 2000), have been attributed to ENSO (PSA-1) on interannual time scales and to the quasi-biennial component of ENSO and the Madden-Julian-Oscillation (PSA-2), respectively (Mo and Paegle, 2001). The relationship between the PSA indices and the PSI revealed a low relationship to both indices ($r_{PSA-1} \approx 0.2$ and $r_{PSA-2} = 0.06$). In contrast, the individual PCs of the zonal circulation in 200 hPa correlate significantly to the PSA-1 index. Positive PSA phases are associated with a strong PFJ over the western Pacific sector (not shown) and the PSA-1 mode is consistently significantly correlated to the PC3(-) component, which is (by definition) related to split events. Negative PSA events are associated with an enhanced PFJ over the eastern hemisphere, which represents the partly EOF2 variability. It is reasoned that PC3 represents both, AAO as well as PSA variability. However, the connection between the PSA-1 mode and the PSI is canceled out by the PC2 component, which is (as well as the PC3 component) negatively correlated to the PSA-1 mode.

The authors concluded that the strength of the relations between the new PC based SH split jet index and the large-scale modes AAO and ENSO are nonlinear. The highly significant relationship to the AAO highlights the importance of the PFJ variability, which is a determining factor for the split jet formation, while the ENSO and PSA effects are complex and relatively less important.

Interestingly, the SH split jet representation is poor in the Earth System Model (not shown) of the Max-Planck-Institute of Meteorology (MPI-ESM) in the Medium resolution (Giorgetta et al., 2013). A possible reason for this deficiency could be a too strong modeled low-pressure system over the Amundsen Sea (Jungclaus et al., 2013), i.e. the prominent (surface) Amundsen Sea Low (ASL). The underestimated variability in that model leads to significant differences in the representation of the leading EOF patterns in the 700 hPa geopotential height (and thus zonal wind) fields in the MPI-ESM model compared to the ERA-Interim reanalysis (Babian et al., 2016).

An extension of the current work is the investigation of seasonal variations in the PSI. In the context of a positive summertime trend in the AAO due to ozone depletion, it is likely that the PSI exhibits significant trends at least on seasonal time scales. Furthermore, the potential of a higher temporal resolved index will be explored. A daily index would be desirable to describe the processes connected to Blocking activity over the Australia / New Zealand sector. These options are currently being investigated and the results will be published in a follow-up study.

Data availability. The ERA-Interim reanalysis data used in this article are freely available from the ECMWF (https://www.ecmwf.int/en/research/climate-reanalysis/era-interim). The climate indices are available from NOAA (http://www.noaa.gov/).

Acknowledgements. The authors appreciate extensive discussion with Prof. Dr. Henning Rust on the statistical concepts used in this study and PD Dr. Peter Névir for comments and insightful discussion on climate dynamics. Thanks are also due to two anonymous reviewers for careful reading the manuscript and for constructive comments.

References

Babian, S., Rust, H. W., Grieger, J., and Cubasch, U.: Representation of the Antarctic Oscillation and related precipitation in the MPI Earth System Model, Meteorol. Z., 17, 12 635, doi:10.1127/metz/2016/0661, 2016.

Bals-Elsholz, T. M., Atallah, E. H., Bosart, L. F., Wasula, T. a., Cempa, M. J., and Lupo, a. R.: The wintertime southern hemisphere split jet: Structure, variability, and evolution, Journal of Climate, 14, 4191–4215, doi:10.1175/1520-0442(2001)014<4191:TWSHSJ>2.0.CO;2, 2001.

Bracegirdle, T. J. and Marshall, G. J.: The reliability of antarctic tropospheric pressure and temperature in the latest global reanalyses, Journal of Climate, 25, 7138–7146, doi:10.1175/JCLI-D-11-00685.1, 2012.

Carvalho, L., Jones, C., and Ambrizzi, T.: Opposite phases of the Antarctic Oscillation and relationships with intraseasonal to interannual activity in the tropics during the austral summer, J. Climate, 18, 702–718, 2005.

Chen, B., Smith, S. R., and Bromwich, D. H.: Evolution of the Tropospheric Split Jet over the South Pacific Ocean during the 1986–89 ENSO Cycle, Monthly Weather Review, 124, 1711–1731, doi:10.1175/1520-0493(1996)124<1711:EOTTSJ>2.0.CO;2, 1996.

Dee, D. P., Uppala, S. M., Simmons, A. J., Berrisford, P., Poli, P., Kobayashi, S., Andrae, U., Balmaseda, M. A., Balsamo, G., Bauer, P., Bechtold, P., Beljaars, A. C. M., van de Berg, L., Bidlot, J., Bormann, N., Delsol, C., Dragani, R., Fuentes, M., Geer, A. J., Haimberger, L., Healy, S., Hersbach, H., Holm, E. V., Isaksen, L., Kållberg, P., Koehler, M., Matricardi, M., McNally, A. P., Monge-Sanz, B. M., Morcrette, J.-J., Park, B.-K., Peubey, C., de Rosnay, P., Tavolato, C., Thepaut, J.-N., and Vitart, F.: The ERA-Interim reanalysis: configuration and performance of the data assimilation system, Quart. J. Roy. Meteor. Soc., 137, 553–597, doi:10.1002/qj.828, 2011.

Ding, Q., Steig, E. J., Battisti, D. S., and Wallace, J. M.: Influence of the Tropics on the Southern Annular Mode, Journal of Climate, 25, 6330–6348, doi:10.1175/JCLI-D-11-00523.1, https://doi.org/10.1175/JCLI-D-11-00523.1, 2012.

Fyfe, J. C.: Separating extratropical zonal wind variability and mean change, Journal of Climate, 16, 863–874, doi:10.1175/1520-0442(2003)016<0863:SEZWVA>2.0.CO;2, 2003.

Gallego, D., Ribera, P., Garcia-Herrera, R., Hernandez, E., and Gimeno, L.: A new look for the Southern Hemisphere jet stream, Climate Dynamics, 24, 607–621, doi:10.1007/s00382-005-0006-7, http://link.springer.com/10.1007/s00382-005-0006-7, 2005.

Galvin, J. F. P.: The weather and climate of the tropics Part 2 –The subtropical jet streams, Weather, 62, 295–299, doi:10.1002/wea.65, http://dx.doi.org/10.1002/wea.65, 2007.

Giorgetta, M. A., Jungclaus, J., Reick, C. H., Legutke, S., Bader, J., Böttinger, M., Brovkin, V., Crueger, T., Esch, M., Fieg, K., Glushak, K., Gayler, V., Haak, H., Hollweg, H.-D., Ilyina, T., Kinne, S., Kornblueh, L., Matei, D., Mauritsen, T., Mikolajewicz, U., Mueller, W., Notz, D., Pithan, F., Raddatz, T., Rast, S., Redler, R., Roeckner, E., Schmidt, H., Schnur, R., Segschneider, J., Six, K. D., Stockhause, M., Timmreck, C., Wegner, J., Widmann, H., Wieners, K.-H., Claussen, M., Marotzke, J., and Stevens, B.: Climate and carbon cycle changes from 1850 to 2100 in MPI-ESM simulations for the Coupled Model Intercomparison Project phase 5, J. Adv. Model. Earth Syst., 5, 572–597, doi:10.1002/jame.20038, 2013.

Hannachi, A., Jolliffe, I. T., and Stephenson, D. B.: Empirical orthogonal functions and related techniques in atmospheric science: A review, Int. J. Climatol., 27, 1119–1152, 2007.

Hendon, H. H., Thompson, D. W. J., and Wheeler, M. C.: Australian Rainfall and Surface Temperature Variations Associated with the Southern Hemisphere Annular Mode, J. Climate, 20, 2452–2467, 2007.

Inatsu, M. and Hoskins, B. J.: The seasonal and wintertime interannual variability of the split jet and the storm-track activity minimum near New Zealand, Journal of the Meteorological Society of Japan, 84, 433–445, doi:10.2151/jmsj.84.433, 2006.

Jolliffe, I. T.: Principal Component Analysis, Springer Series in Statistics, Springer, New York, 3rd edn., 2002.

Jungclaus, J. H., Fischer, N., Haak, H., Lohmann, K., Marotzke, J., Matei, D., Mikolajewicz, U., Notz, D., and von Storch, J. S.: Characteristics of the ocean simulations in the Max Planck Institute Ocean Model (MPIOM) the ocean component of the MPI-Earth system model, J. Adv. Model. Earth Syst., 5, 422–446, doi:10.1002/jame.20023, http://dx.doi.org/10.1002/jame.20023, 2013.

Karoly, D. J.: Southern hemisphere circulation features associated with El Niño-Southern Oscillation events, Journal of Climate, 2, 1239–1252, 1989.

Kitoh, A.: Tropical Influence on the South Pacific Double Jet Variability, Proc. NIPR Symp. Polar Meteorol. Glaciol., 8, 34–45, 1994.

Limpasuvan, V. and Hartmann, D. L.: Eddies and the annular modes of climate variability, Geophysical Research Letters, 26, 3133–3136, doi:10.1029/1999gl010478, 1999.

Lorenz, D. J. and Hartmann, D. L.: Eddy–Zonal Flow Feedback in the Southern Hemisphere, Journal of the Atmospheric Sciences, 58, 3312–3327, doi:10.1175/JAS4005.1, 2001.

Mechoso, C. R., O'Neill, A., Pope, V. D., and Farrara, J. D.: A study of the stratospheric final warming of 1982 in the southern hemisphere, Quarterly Journal of the Royal Meteorological Society, 114, 1365–1384, doi:10.1002/qj.49711448402, http://dx.doi.org/10.1002/qj.49711448402, 1988.

Mo, K. C.: Relationships between Low-Frequency Variability in the Southern Hemisphere and Sea Surface Temperature Anomalies, J. Climate, 13, 3599–3610, 2000.

Mo, K. C. and Higgins, R. W.: The Pacific–South American Modes and Tropical Convection during the Southern Hemisphere Winter, Monthly Weather Review, 126, 1581–1596, doi:10.1175/1520-0493(1998)126<1581:TPSAMA>2.0.CO;2, https://doi.org/10.1175/1520-0493(1998)126<1581:TPSAMA>2.0.CO;2, 1998.

Mo, K. C. and Paegle, J. N.: The Pacific–South American modes and their downstream effects, International Journal of Climatology, 21, 1211–1229, doi:10.1002/joc.685, http://dx.doi.org/10.1002/joc.685, 2001.

Mo, K. C., Pfaendtner, J., and Kalnay, E.: A GCM Study on the Maintenance of the June 1982 Blocking in the Southern Hemisphere, Journal of the Atmospheric Sciences, 44, 1123–1142, doi:10.1175/1520-0469(1987)044<1123:AGSOTM>2.0.CO;2, 1987.

North, G. R., Bell, T. L., Cahalan, R. F., and Moeng, F. J.: Sampling errors in the estimation of empirical orthogonal functions, Mon. Wea. Rev., 110, 699–706, doi:10.1175/1520-0493(1982), 1982.

Pook, M. J., Risbey, J. S., McIntosh, P. C., Ummenhofer, C. C., Marshall, A. G., and Meyers, G. A.: The Seasonal Cycle of Blocking and Associated Physical Mechanisms in the Australian Region and Relationship with Rainfall, Monthly Weather Review, 141, 4534–4553, doi:10.1175/MWR-D-13-00040.1, 2013.

Taljaard, J.: Synoptic Meteorology of the Southern Hemisphere, Meteorological Monographs, Boston, 13 edn., 1972.

Thompson, D. and Wallace, J. M.: Annular modes in the extratropical circulation. Part I: Month-to-month variability, J. Climate, 13, 1000–1016, 2000.

Trenberth, K. F. and Mo, K. C.: Blocking in the Southern Hemisphere, Monthly Weather Review, 113, 3–21, doi:10.1175/1520-0493(1985)113<0003:BITSH>2.0.CO;2, 1985.

Wilks, D. S.: Statistical methods in the atmospheric sciences, Academic Press, San Diego, CA, 3rd edn., 2011.

Yang, X. and Chang, E. K. M.: Variability of the Southern Hemisphere Winter Split Flow – A Case of Two-Way Reinforcement between Mean Flow and Eddy Anomalies, Journal of Atmospheric Sciences, 63, 634–650, doi:10.1175/JAS3643.1, 2006.